Rotational motion of methane within the confines of zeolite NaCa*A*: Molecular dynamics and *ab initio* calculations

A. V. Anil Kumar,[1] S. Yashonath,[1,2] Marcel Sluiter,[3] and Yoshiyuki Kawazoe[3]
[1]*Solid State and Structural Chemistry Unit, Indian Institute of Science, Bangalore 560 012, India*
[2]*Center for Condensed Matter Theory, Indian Institute of Science, Bangalore 560 012, India*
[3]*Institute for Materials Research, Tohoku University, Sendai 980-8577, Japan*
(Received 19 July 2001; published 17 December 2001)

Molecular dynamics simulation of a five-site model of methane within zeolite NaCa*A* and *ab initio* calculations have been reported. Methane shows a preferential orientation during its passage through the eight-ring window. Partial freezing of certain rotational degrees of freedom is observed during the passage of methane through the eight-ring window, which acts as a bottleneck for diffusion of methane. Both the orientation and the rotational motion of methane and its experimental verification can indicate the accuracy of the intermolecular potential between methane and zeolite employed in this study. Intracage motion of methane shows that methane performs a rolling motion rather than a sliding motion within the supercage.

DOI: 10.1103/PhysRevE.65.011203 PACS number(s): 66.10.−x, 51.20.+d, 81.05.Rm

I. INTRODUCTION

Diffusion in gases, liquids, and solids has been studied widely for more than a century [1]. But there has been an increasing interest in the diffusion of fluids in porous media for the last decade and a half [2,3]. Porous materials are of considerable practical importance in catalytic and separation processes mainly due to their high specific area and size selective adsorption [4]. Transport through porous materials mainly occurs through diffusion and often affects and controls the reaction and its products [5]. So a detailed understanding of the complexities of diffusional behavior in porous media is essential for the development and design of catalytic and adsorption processes.

Zeolites are a class of crystalline porous materials with a uniform micropore size. Experimental and theoretical investigations reveal a variety of interesting and surprising properties of fluids confined in zeolites [6]. The study of adsorption of hydrocarbons within zeolitic pores are of considerable importance to the petrochemical industry. Among other uses, zeolites are used in chemical transformation of hydrocarbons including alkanes and aromatics. Cracking of linear and branched alkanes is one of the important applications of zeolites. Another important application is that of separation of mixtures of hydrocarbons. Methane is the simplest prototype of the alkanes in spite of the fact that it lacks the torsional degrees of freedom that become important as the chain length increases. Recently, the existence of translational-orientational coupling during the passage of methane through the bottleneck provided by the eight-ring window of zeolite *A* was reported [7]. Here, we report a detailed molecular dynamics (MD) study in zeolite NaCa*A* and an *ab initio* study of methane in the dealuminated cage of zeolite *A*. The analysis of the MD trajectories is carried out to understand the reasons for strong orientational preference during the passage of methane through the bottleneck reported recently and to look at the role of rotational motion especially during the motion of methane inside the α-cage.

II. STRUCTURE OF ZEOLITE NaCa*A*

Zeolites are porous aluminosilicates consisting of SiO_4 and AlO_4 tetrahedra interconnected through shared vertices: the oxygen atoms. The structure of zeolite NaCa*A* reported by Pluth and Smith [8] has been used in the present work. The space group is $Fm\bar{3}c$ with a unit-cell dimension $a = 24.555$ Å. The unit-cell composition is $Na_{32}Ca_{32}Al_{96}Si_{96}O_{384}$. The sodium and calcium ions occupy positions close to the center of the six-ring windows. There are eight supercages in one unit cell of NaCa*A* and these are connected to each other in an octahedral fashion. The approximate diameter of the supercages is 11.4 Å. They are interconnected through eight-ring windows of diameter 4.5 Å.

III. COMPUTATIONAL DETAILS

A. Classical simulations

Molecular dynamics simulations of methane molecules confined in zeolite NaCa*A* have been carried out in the microcanonical ensemble. The simulation cell consists of $(2\times2\times2)$ unit cells of zeolite NaCa*A* with 64 methane molecules at a loading of one molecule per supercage. Cubic periodic conditions are used in all three directions. Zeolite atoms are not included in the integration scheme. The rotation of the molecules are modeled using quarternion formalism. Both translational and rotational equations are integrated using the Gear predictor-corrector algorithm. An integration time step of 1 fs was found to be adequate. The temperature of the run is 150 K. A production run of 1 ns duration has been used in obtaining averages after an initial equilibration period of 200 ps. The intermolecular potential parameters between methane and zeolite atoms are taken from the literature [9,10]. The Lorentz-Berthelot combination rule is used to get the cross or mixed terms. The potentials are of the [6–12] Lennard-Jones form

$$\phi(r) = 4\epsilon\left[\left(\frac{\sigma}{r}\right)^{12} - \left(\frac{\sigma}{r}\right)^{6}\right].$$

TABLE I. Potential parameters for CH_4-CH_4 and CH_4-NaCa*A* interactions.

Type	σ (Å)	ϵ (kJ/mol)
C-C	3.350	0.4054
H-H	2.813	0.0683
C-O	2.950	0.7229
C-Na	3.360	0.1261
C-Ca	3.350	1.9671
H-O	2.682	0.2968
H-Na	3.092	0.0517
H-Ca	3.082	0.8076

A five-site model was used for methane. The methane molecules were assumed to interact only with the oxygen atoms of the zeolite framework. The Si and Al atoms in the zeolite host are largely shielded by the surrounding oxygens, thus making the short-range interaction of these with the guest molecules insignificant. Table I lists the potential parameters for the methane-methane and methane-zeolite interactions.

B. *Ab initio* calculations

Calculations were carried out using the all-electron full-potential mixed-basis method [11] within the local density approximation of density functional theory. In this method wave functions are represented on a basis of truncated atomic orbitals and plane waves. The cutoff energy of 288 eV corresponding to 20 479 plane waves was employed while the number of atomic orbitals was 465. The one-electron picture was attained by using the Perdew-Zunger exchange-correlation potential [12] with self-interaction corrections. A standard cage size of 12.2775 Å, as given by x-ray diffraction [8], consisting of 24 Si atoms and 48 O atoms was used; see Fig. 1. The reciprocal space integrations were carried out using the γ point only because the cage is large and because there is a large band gap. The C-H distance employed for methane is the experimentally determined value of 1.09 Å [13]. The mixed-basis method gives a C-H distance with about 2.6% error that is acceptable in view of the local density approximation. These calculations are computer intensive and were carried out on the Hitachi SR8000 supercomputer. Calculations were performed for both (2+2) and (1+3) orientations in ten intervals from the cage center to the window positions.

IV. RESULTS AND DISCUSSION

A. Energetics and structure

The average values of the thermodynamic properties are listed in Table II.

The center of mass-center of cage radial distribution function (r.d.f.) is shown in Fig. 2(a) as a function of the distance from the cage center. As is clear from the figure a predominant peak is observed at 3.7 Å from the cage center. This peak is due to the strong interaction between the sorbate and the inner surface of the α-cage. Cohen de Lara and Khan [14] have reported neutron scattering studies of methane in zeolite *A* where they found that around 200 K the region near the periphery of the cage is populated predominantly. At higher temperatures, the region near the center of the cage also begins to get populated.

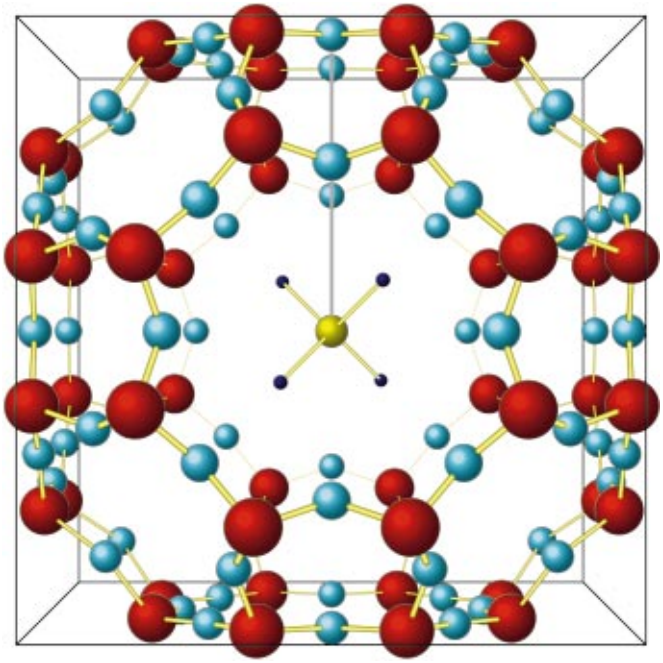

FIG. 1. (Color) Zeolite $Si_{24}O_{48}$ cage used for the mixed-basis calculations; the methane molecule is in the (2+2) position at the center of the cage; it is moved in 10 steps toward the window center along the thick gray line. Color coding for atoms: Si, red; O, light blue; C, yellow; and H, dark blue.

The guest-guest r.d.f. between the center of mass–center of mass (c.o.m-c.o.m) of methane is shown in Fig. 2(b). There is a prominent peak at 4.1 Å. This indicates that even at the low concentration of one molecule per cage pairs of methane molecules exist. There is no second peak observed in the c.o.m-c.o.m r.d.f, which suggests that no clusters involving more than first shell neighbors exist.

B. Dynamical properties

Earlier investigations [15] into diffusion of sorbates in zeolites such as zeolite *A* and faujasite suggest that the diffusion process may be subdivided into two subprocesses: (i) intercage diffusion and (ii) intracage diffusion. The latter consists of motion within the supercage and primarily involves hopping from one physisorption site to another. The

TABLE II. Average properties of CH_4 in NaCa*A* from the molecular dynamics run.

Average property	CH_4 in NaCa*A*
$\langle T_{trans} \rangle$ (K)	151.31
$\langle T_{rot} \rangle$ (K)	151.16
$\langle U_{tot} \rangle$ (kJ/mol)	−15.0464

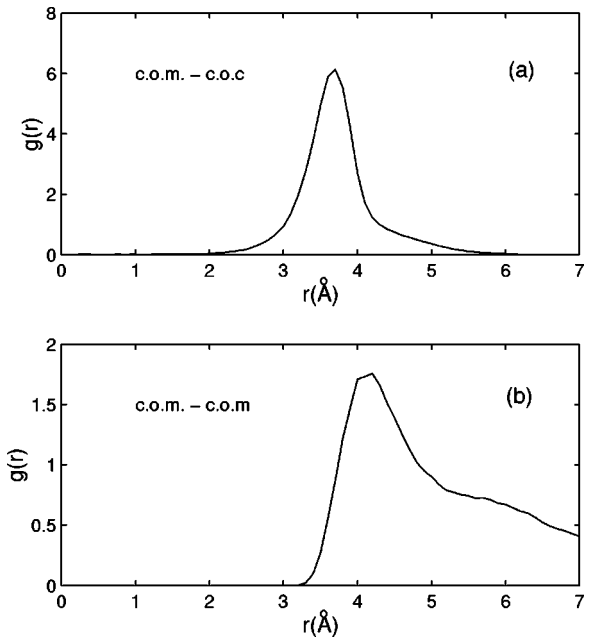

FIG. 2. (a) Center of mass–center of cage radial distribution function as a function of the distance from the cage center and (b) the center of mass–center of mass radial distribution function of methane.

other subprocess is the intercage diffusion that consists of hops from one supercage to another through the narrower window. This subprocess is often the rate determining step for diffusion. Recent investigations [7] reveal that methane preferentially orients itself before passing through the eight-ring window in zeolite *A*.

1. Intercage diffusion and orientation of methane

If θ is the angle between $\hat{\mathbf{n}}$, the vector perpendicular to the eight-ring window, and the C—H bond, then $0<\theta<\theta_{T_d}$. Here, $\theta_{T_d}=109.5°$. The smallest of the four θ's, θ_{min}, between the four C—H bonds and $\hat{\mathbf{n}}$ is indicative of the orientation methane has with respect to $\hat{\mathbf{n}}$. θ_{min} should necessarily lie in the interval $(0,\theta_{T_d}/2)$. If $0<\theta<\theta_{T_d}/4$, the methane orientation is said to be (1+3) and if $\theta_{T_d}/4<\theta<\theta_{T_d}/2$, it is said to be (2+2), since in the former case one hydrogen gets past the narrow window and this is followed by three other hydrogens or vice versa. In the case of (2+2) orientation two hydrogens get past the window and these are followed by two other hydrogens. It was found that (2+2) is the preferred orientation (80%) when the c.o.m. of methane is in the plane of the eight-ring window. In order to obtain an estimate of $\zeta=\langle\cos\theta_{min}\rangle$, we averaged this quantity over all intercage crossover events. This is shown in Fig. 3(a) as a function of the distance d from the plane of the eight-ring window. d is defined to be negative before it passes through the window. Note that at $\theta=\theta_{T_d}/4$, $\cos\theta=0.888$. A horizontal dashed line has been shown in Fig. 3(a) corresponding to this. It is seen that the average value of ζ is ≈ 0.8 or $\theta_{min}\approx 36.8°$ suggesting a (2+2) orientation. Figure 3(b) shows

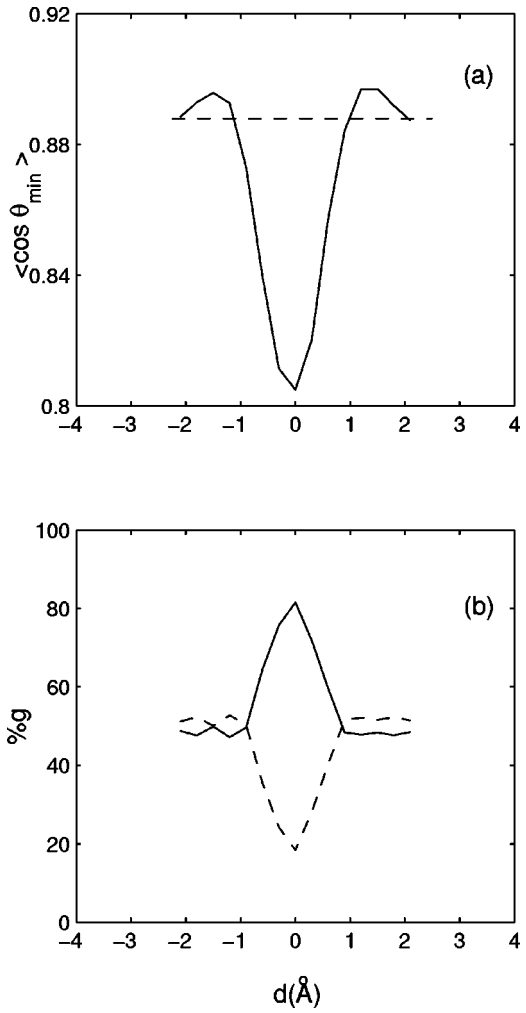

FIG. 3. (a) The average value of cos θ as a function of perpendicular distance d from the window plane and (b) percentage of molecules in (2+2) (solid line) and (1+3) (dashed line) orientations.

the percentage of molecules in (2+2) (solid line) and (1+3) (dashed line) orientations. Strong preference for (2+2) is seen at the window plane.

Figure 4(a) shows U_{gh} obtained from simple calculation of interaction energies along a straight line connecting the centers of two cages and passing through the window center. These are termed static calculations since they are not averaged over MD trajectories. Further, the methane orientation is such that one hydrogen points towards the eight-ring window instead of three hydrogens pointing towards the window. When the particle approaches within 2 Å of the window plane, the (2+2) and (1+3) orientations begin to differ in U_{gh}, with the former having a more favorable interaction.

Figure 4(b) shows a plot of U_{gh} averaged over all MD *trajectories* during cage-to-cage migration. (There were 1013 crossover events during the 1 ns simulation run.) It is seen that the energy for (2+2) and (1+3) differs only for $|d|<0.8$ Å. The difference in the two curves [Figs. 4(a) and 4(b)] arises from the difference in the trajectories between the static (a) and MD averaged calculations (b). This is because in an MD run the trajectory of methane in close prox-

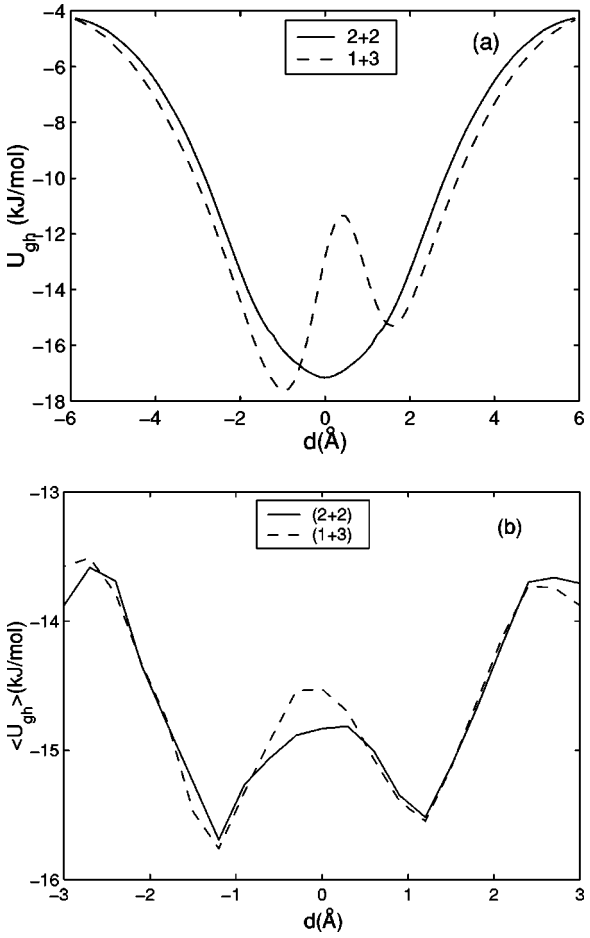

FIG. 4. (a) The variation of the guest-host intermolecular interaction energy along a straight line connecting the centers of two cages and passing through the window center vs perpendicular distance d from the window plane. For the (1+3) orientation, a single hydrogen was pointing towards the eight-ring window. Note that the force on methane at $d=0$ is nonzero for (1+3) orientation as expected. (b)A plot of U_{gh} averaged over all MD trajectories during cage-to-cage migration. Here, we do not distinguish between a single hydrogen pointing towards window and the other orientation in which a single hydrogen is pointing away from window and, therefore, the force at $d=0$ is zero.

imity to the inner surface of the α-cage. This is not the case for a line connecting two cage centers [Fig. 4(a)]. Further, here the dot product does not distinguish between the orientation in which one hydrogen points towards the window and three hydrogens point towards the window. As a result the curve is essentially symmetric with respect to $d=0$ plane (the window plane). In case of MD averaged U_{gh} both (1+3) and (2+2) exhibit a local maximum at the window plane [Fig. 4(b)] as compared to a minimum for (2+2) along the line interconnecting the two cage centers. The difference in U_{gh} between (1+3) and (2+2) is also significantly lower.

2. Intermolecular potential and alkane-zeolite system

Methane as well as the methyl group and methylene groups of hydrocarbons are approximately similar in size when they are modeled in terms of a single site (united atom model). According to the optimized potentials of Jorgensen for liquid hydrocarbons [16], the Lennard-Jones parameters for the united atom model are: $\sigma_{CH_4}=3.73$ Å, $\sigma_{CH_3}=3.775$–3.91 Å, and $\sigma_{CH_2}=3.85$–3.905 Å. The eight-ring window has a diameter closely comparable to these σ values. Some recent studies by Sahimi and co-workers have attempted to look at the influence of variation in σ value for methane (united atom model) on the separation factors [17,18]. It is interesting to note that these studies of Sahimi and co-workers did reveal the strong influence of the choice of σ on separation factors. It is clear, however, that a single-site model will be inadequate in studies such as the present one, where orientations influence the guest-zeolite energy and other dynamics.

We, therefore, focus on the five-site models for methane, but these arguments are equally applicable to various hydrocarbon groups such as CH_3, CH_2, and CH. The results for methane, namely, whether (2+2) or (1+3) is preferable might depend crucially on the choice of the Lennard-Jones parameters, especially the σ value (σ_{HO} and σ_{CO}) that is the used in these simulations. In the literature there have been few accurate estimates of parameters between the guest species and zeolite except that of Pellenq and Nicholson for rare gases within silicalite-1 zeolite [19]. There have been some attempts to distinguish between different choices for the σ_{OC} and σ_{HO} parameters between methane, methyl, and methylene on one hand and oxygen of the zeolite on the other. But these methods are indirect [17,18]. If experimental techniques such as nuclear magnetic resonance (NMR) can distinguish between the (2+2) and (1+3) orientations and the observed results agree with the present study, it might mean that the values of σ between the hydrogens and carbons on the one hand and the oxygen on the other are reasonably accurate. Any disagreement will call for refinement of these parameters. One way of checking the validity of the choice of the σ values employed by us in the classical MD simulations in this study is to estimate the energy difference between the (2+2) and (1+3) orientations from *ab initio* calculations. The cluster of the zeolite employed by us in the *ab initio* calculations is shown in Fig. 1. The values of σ and ϵ parameters that are appropriate may depend on the environment in which a guest molecule is placed, as pointed out by Derouane [20]. Such behavior necessitates more *ab initio* MD studies.

3. Ab initio mixed-basis calculations

Ab initio calculations of van der Waals systems such as the adsorption of small hydrocarbon molecules in zeolite are very challenging. Local density calculations do not generally provide highly accurate estimates of van der Waals interactions because errors in the approximated exchange-correlation potential are not dwarfed by electronic overlap or Coulombic terms as is the case in covalent, metallic, and ionic interactions. Fortunately, the self-interaction correction [12] was found to give reasonable results for the zeolite-methane interaction.

Figure 5 shows the potential energy of a methane molecule in a zeolite supercage along a straight line path from

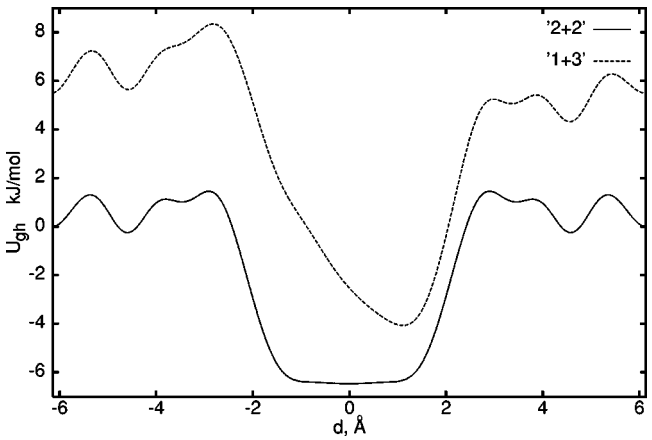

FIG. 5. Potential energy of a methane molecule along a straight line connecting the centers of two cages and passing through the window center vs perpendicular distance d from the window plane for the (2+2) and (1+3) orientations (solid and dashed lines, respectively). For the (1+3) orientation a lone hydrogen atom points towards (away from) the window for positive (negative) distances.

cage center to cage center through a window as computed with the mixed-basis method. The trajectory is identical to that shown for Fig. 4(a). The energy of a methane in the (2+2) orientation at the cage center is selected as the reference point. Clearly the (2+2) orientation is favored over the (1+3) position at all positions along this path. Even at the cage center, the energy difference between (2+2) and (1+3) orientations is found to be large, about 5.5 kJ/mol. The (2+2) orientation features a wide potential well of about 7 kJ/mol with a width of about 2 Å on either side of the window. It should be noted that while the (2+2) orientation is symmetric with respect to the window, the (1+3) orientation is not. For positive (negative) distances, the single hydrogen atom points towards (away from) the window. A potential well exists for the (1+3) orientation as well, but it has a minimum that does not coincide with $d=0$, the position where the window is located. It occurs when the single hydrogen atom is right at the window while the carbon and remaining three hydrogen atoms are farther removed from the window. The bottom of the (1+3) potential well is not flat like the (2+2) well, but rather pointed and lies about 2.4 kJ/mol above the bottom of the (2+2) well.

These results agree with the classical calculations in regard to their most important feature, the occurrence of a deep potential well in the vicinity of the window center with a deeper and wider well for the (2+2) than for the (1+3) orientation, as can be seen by comparing Fig. 5 with Fig. 4(a). However, in the details there are some differences: The *ab initio* calculation gives a single minimum for the (1+3) orientation, and it also gives that the (2+2) is always favored over the (1+3) orientation. At the cage center the classical potential gives an insignificant energy difference between the two orientations, while the *ab initio* result favors the (2+2) by about 5.5 kJ/mol. When the carbon of CH_4 is located at the window center, the difference in energies between (1+3) and (2+2) is about 4 kJ/mol from *ab initio* as well as classical static energy calculations. The well depths defined as the difference in energy between the cage and the window

TABLE III. Average value of $|\omega|_{d=0}$, $|\omega_{C_2}|_{d=0}$, and $|\omega_{C_3}|_{d=0}$ for all cage to cage crossovers (total), (2+2) orientation, and (1+3) orientation.

	$\lvert\omega\rvert_{d=0}$ (fs^{-1})	$\lvert\omega_{C_2}\rvert_{d=0}$ (fs^{-1})	$\lvert\omega_{C_3}\rvert_{d=0}$ (fs^{-1})
Total	3.013×10^{-4}	2.379×10^{-4}	1.848×10^{-4}
(2+2)	2.981×10^{-4}	2.634×10^{-4}	1.396×10^{-4}
(1+3)	3.138×10^{-4}	1.883×10^{-4}	2.511×10^{-4}

agree reasonably: for the (1+3) orientation, in particular, the *ab initio* and the classical result are, respectively, 10 and 13 kJ/mol, while for the (2+2) orientation the results are 7 and 13 kJ/mol. This supports the classical calculations and indicates that the intermolecular potential functions and σ parameters for the interaction between the methane and the zeolite Na*A* are at least predicting the trends correctly.

4. Partial freezing of certain rotational degrees of freedom

During the passage of methane through the bottleneck, preferential orientation observed earlier and the difference in energy between (2+2) and (1+3) would necessitate that the corresponding symmetry be maintained: a (2+2) methane can only rotate along a C_2 rotation axis if its orientation with respect to the window is to remain unchanged; any rotation around C_3 will immediately alter the orientation of methane with respect to $\hat{\mathbf{n}}$, the unit vector perpendicular to the window plane. Similarly, only a rotation around the C_3 axis that is nearly parallel to $\hat{\mathbf{n}}$ will not alter the (1+3) methane with respect to $\hat{\mathbf{n}}$. It is, therefore, expected that for the (2+2) orientation at the window plane the rotational component along any direction except the C_2 axis closest to $\hat{\mathbf{n}}$ needs to freeze or at least slow down. In other words, the C_2 axis whose angle with $\hat{\mathbf{n}}$ is smallest should show the largest component of the angular velocity. Table III lists the magnitudes of total angular velocity and some of its components for methane whose center of mass is within (± 2 Å) from the window plane. The components are along the C_2 axis closest to $\hat{\mathbf{n}}$, ω_{C_2}, and along the C_3 axis closest to $\hat{\mathbf{n}}$, ω_{C_3}, for methane in the (2+2) and (1+3) orientation. It is seen that the magnitude is indeed larger along C_2 axis (than along the C_3 axis) for methane in the (2+2) orientation and the C_3 axis (in comparison to the C_2 axis) for methane in the (1+3) orientation. This suggests that methane passing through the window prefers to maintain the symmetry with respect to the window plane (or the vector perpendicular to it). This is because the energy cost associated with such a change would be significant.

5. Intracage diffusion: Rolling or sliding methane?

We did not find any preferential orientation for methane in the supercage. In order to look at the nature of motion within the cage we analyzed trajectories that were at least 2 Å away from the window plane.

First, we computed the dot products $\hat{\boldsymbol{\omega}}\cdot\hat{\boldsymbol{v}}$, $\hat{\boldsymbol{\omega}}\cdot\hat{\boldsymbol{r}}$, and $\hat{\boldsymbol{v}}\cdot\hat{\boldsymbol{r}}$, where $\hat{\boldsymbol{\omega}}$, $\hat{\boldsymbol{v}}$, and $\hat{\boldsymbol{r}}$ are the unit vectors along the angular velocity, velocity of c.o.m. and the vector from the resident cage center to the center of mass of methane. They are $\hat{\boldsymbol{\omega}}\cdot\hat{\boldsymbol{v}}=0.499$ ($\theta=60.06°$), $\hat{\boldsymbol{\omega}}\cdot\hat{\boldsymbol{r}}=0.388$ ($\theta=67.11°$), and $\hat{\boldsymbol{v}}\cdot\hat{\boldsymbol{r}}=0.228$ ($\theta=76.79°$). This shows that there is a large component of angular velocity perpendicular to the linear velocity. The radial vector $\hat{\boldsymbol{r}}$ is more or less perpendicular to both linear velocity and angular velocity. Now consider the vectors:

$$\boldsymbol{u}_{\mathbf{v}_\parallel}=\hat{\boldsymbol{v}}-(\hat{\boldsymbol{v}}\cdot\hat{\boldsymbol{r}})\hat{\boldsymbol{r}},$$

$$\boldsymbol{u}_{\mathbf{v}_\perp}=\hat{\boldsymbol{r}}\times\hat{\boldsymbol{u}}_{\mathbf{v}_\parallel}.$$

Note that $\hat{\boldsymbol{r}}$, $\hat{\boldsymbol{u}}_{\mathbf{v}_\perp}$, and $\hat{\boldsymbol{u}}_{\mathbf{v}_\parallel}$ now form three vectors that are mutually perpendicular to each other. We have calculated the angular velocity components along these three directions: $\omega_r=0.000\,130\,5$/fs, $\omega_{u_{v_\perp}}=0.000\,274\,9$/fs, and $\omega_{u_{v_\parallel}}=0.000\,141\,4$/fs. It is seen that $\omega_{u_{v_\perp}}$ is the largest in magnitude. This suggests that rolling motion contributes significantly to the motion of methane. Earlier simulations have shown that methane exhibits a large preference for the periphery of the supercage [21]. The inner surface of supercage of Na*A* zeolite has a reasonable surface roughness. This gives a picture of methane rolling on the surface of the supercage rather than sliding. This may be compared with the skating (creeping) motion of benzene found by Auerbach [22] in zeolite Na*Y*. Methane being globular in shape and well known to exhibit an orientationally disordered plastic crystalline state, can easily roll rather than slide. Benzene whose molecular geometry is highly anisotropic cannot easily roll.

V. CONCLUSIONS

The diffusion of methane within zeolite NaCa*A* consists of two parts: intercage and intracage motion. In the former, methane shows preferential orientation during its passage through the bottleneck, the eight-ring window interconnecting two supercages. Both mixed-basis *ab initio* and classical empirical Lennard-Jones potential suggest that the (2+2) orientation has a lower energy at the eight-ring window by about 3.5–5.8 kJ/mol. It is also seen that partial freezing of rotational degrees of freedom occurs along directions that change the symmetry of methane with respect to the vector normal to the eight-ring window plane. During intracage motion, it is seen that methane rolls rather than slides along the inner wall of the supercage.

ACKNOWLEDGMENTS

Financial support from Department of Science & Technology, New Delhi for purchase of computers is gratefully acknowledged. We wish to acknowledge JSPS for financial support to S.Y. to visit IMR Sendai where part of this work was carried out. The authors also gratefully acknowledge the staff at the Computer Center at IMR-Tohoku University for time on the Hitachi SR8000 supercomputer.

[1] W. Jost, *Diffusion in Solids, Liquids, and Gases* (Academic Press, New York, 1960).
[2] J. Kärger and D. M. Ruthven, *Diffusion in Zeolites and other Microporous Solids* (Wiley, New York, 1992).
[3] S. P. Bates and R. A. van Santen, Adv. Catal. **42**, 1 (1998).
[4] R. M. Barrer, *Zeolites and Clay Minerals as Sorbents and Molecular Sieves* (Academic Press, London, 1978).
[5] J. M. Thomas and W. M. Thomas, *Principles and Applications of Heterogenous Catalysis* (VCH, Weinheim, Germany, 1997).
[6] F. J. Keil, R. Krishna, and M.-O. Coppens, Rev. Chem. Eng. **16**, 71 (2000).
[7] R. Chitra, A. V. Anil Kumar, and S. Yashonath, J. Chem. Phys. **114**, 11 (2001).
[8] J. J. Pluth and J. V. Smith, J. Am. Chem. Soc. **102**, 4704 (1980).
[9] S. Murad and K. E. Gubbins, ACS Symp. Ser. **86**, 62 (1978).
[10] P. Santikary and S. Yashonath, J. Chem. Soc., Faraday Trans. **88**, 1063 (1992).
[11] M. Sluiter, K. Ohno, Y. Maruyama, and Y. Kawazoe, Comp. Phys. Comm. (to be published).
[12] J. P. Perdew and A. Zunger, Phys. Rev. B **23**, 5048 (1981).
[13] J. H. Callomon *et al.*, in *Structure Data of Free Polyatomic Molecules* in *Landolt-Börnstein Numerical Data and Functional Relationships in Science and Technology*, edited by K.-H. Hellwege, New Series, Group II, Vol. 7, (Springer-Verlag, Berlin, 1976).
[14] E. Cohen de Lara and R. Khan, J. Phys. (Paris) **42**, 1029 (1981).
[15] S. Yashonath and P. Santikari, J. Phys. Chem. **87**, 3849 (1993).
[16] W. L. Jorgensen, J. D. Madura, and C. J. Swenson, J. Am. Chem. Soc. **106**, 6638 (1984).
[17] L. Xu, M. G. Sedigh, M. Sahimi, and T. T. Tsotsis, Phys. Rev. Lett. **80**, 3511 (1998).
[18] L. Xu, T. T. Tsotsls, and M. Sahimi, J. Chem. Phys. **111**, 3252 (1999).
[19] R. J.-M. Pellenq and D. Nicholson, J. Phys. Chem. **98**, 13339 (1994).
[20] E. G. Derouane, J. Mol. Catal. A: Chem. **134**, 29 (1998).
[21] S. Yashonath, J. M. Thomas, A. K. Nowak, and A. K. Cheetham, Nature (London) **331**, 601 (1988).
[22] F. Jousse, S. M. Auerbach, and D. P. Vercauteren, J. Phys. Chem. B **104**, 2360 (2000).